Growth Differentiation Factor 15 Mediates Systemic Glucose Regulatory Action of T-Helper Type 2 Cytokines

Seong Eun Lee,[1,2] Seul Gi Kang,[1,2] Min Jeong Choi,[1,2] Saet-Byel Jung,[1] Min Jeong Ryu,[3] Hyo Kyun Chung,[1] Joon Young Chang,[1,2] Yong Kyung Kim,[1] Ju Hee Lee,[1] Koon Soon Kim,[1] Hyun Jin Kim,[1] Heung Kyu Lee,[4] Hyon-Seung Yi,[5] and Minho Shong[1]

Diabetes 2017;66:2774–2788 | https://doi.org/10.2337/db17-0333

METABOLISM

T-helper type 2 (Th2) cytokines, including interleukin (IL)-13 and IL-4, produced in adipose tissue, are critical regulators of intra-adipose and systemic lipid and glucose metabolism. Furthermore, IL-13 is a potential therapy for insulin resistance in obese mouse models. Here, we examined mediators produced by adipocytes that are responsible for regulating systemic glucose homeostasis in response to Th2 cytokines. We used RNA sequencing data analysis of cultured adipocytes to screen factors secreted in response to recombinant IL-13. Recombinant IL-13 induced expression of growth differentiation factor 15 (GDF15) via the Janus kinase-activated STAT6 pathway. In vivo administration of α-galactosylceramide or IL-33 increased IL-4 and IL-13 production, thereby increasing GDF15 levels in adipose tissue and in plasma of mice; however, these responses were abrogated in STAT6 knockout mice. Moreover, administration of recombinant IL-13 to wild-type mice fed a high-fat diet (HFD) improved glucose intolerance; this was not the case for GDF15 knockout mice fed the HFD. Taken together, these data suggest that GDF15 is required for IL-13–induced improvement of glucose intolerance in mice fed an HFD. Thus, beneficial effects of Th2 cytokines on systemic glucose metabolism and insulin sensitivity are mediated by GDF15. These findings open up a potential pharmacological route for reversing insulin resistance associated with obesity.

Adipose tissue comprises stromal and vascular cells, including innate and adaptive immune cells, fibroblasts, and endothelial cells, in addition to adipocytes. All cells in adipose tissue participate in regulating systemic glucose metabolism. There are differences in the immune cell composition of adipose tissue between lean and obese individuals. Adipose tissue in lean mice and humans contains a higher proportion of M2/M1 macrophages, which are associated with local production of T-helper type 2 (Th2) cytokines by eosinophils (1). Obesity is associated with local adipose inflammation, which is characterized by dysregulated immune cell function (2). $CD8^+$ T cells play a critical role in high-fat diet (HFD)–induced obesity and adipose inflammation via recruitment and activation of macrophages (3). Adipose-infiltrating macrophages secrete inflammatory cytokines such as tumor necrosis factor-α (TNF-α) and interleukin (IL)-6 (4). Secretion of TNF-α, plasminogen activator inhibitor-1, IL-6, IL-1β, and other inflammatory cytokines by adipose tissues in obese patients is higher than that in lean individuals (5,6). However, regulatory T cells and Th2 cells in adipose tissue suppress inflammatory responses by producing the anti-inflammatory cytokine IL-10 (7,8).

Emerging evidence suggests that the IL-33–driven type 2 innate lymphoid cell (ILC2)/eosinophil axis plays a role in browning of white adipose tissue (WAT), thereby preventing development of obesity (9,10). Eosinophils in adipose tissue are involved in metabolic homeostasis via IL-4/IL-13–mediated reconstitution of macrophages (1). Administration of recombinant IL-4 to mice reduces weight gain and protects them from diet-induced obesity (11). In addition, IL-4 improves the metabolic indices of insulin resistance and

[1]Research Center for Endocrine and Metabolic Diseases, Chungnam National University School of Medicine, Daejeon, Korea
[2]Department of Medical Science, Chungnam National University School of Medicine, Daejeon, Korea
[3]Department of Biochemistry, Chungnam National University School of Medicine, Daejeon, Korea
[4]Graduate School of Medical Science and Engineering, Korea Advanced Institute of Science and Technology, Daejeon, Korea
[5]Department of Internal Medicine, Chungnam National University Hospital, Daejeon, Korea

Corresponding authors: Minho Shong, minhos@cnu.ac.kr, and Hyon-Seung Yi, jmpbooks00@gmail.com.

Received 23 March 2017 and accepted 24 August 2017.

This article contains Supplementary Data online at http://diabetes.diabetesjournals.org/lookup/suppl/doi:10.2337/db17-0333/-/DC1.

improves the action of insulin in liver and muscle in a STAT6-dependent manner (11). Furthermore, IL-13 knockout (KO) mice are glucose intolerant and insulin resistant as a result of dysregulation of hepatic gluconeogenesis (12). Despite this molecular link between the immune system and macronutrient metabolism, how Th2 cytokines in adipose tissue regulate glucose metabolism and insulin sensitivity is not clear.

Evidence suggests that growth differentiation factor 15 (GDF15) is also secreted by adipocytes; this factor is thought to be an adipokine that promotes oxidative function and lipolysis in liver and adipose tissue (13). However, the relationship between GDF15 and the immune microenvironment associated with obesity-induced adipose inflammation has not been characterized, and the factors that regulate GDF15 expression in adipose tissue are unclear. Here, we screened mediators secreted by adipocytes in response to stimulation by Th2 cytokines and examined their role in regulating systemic energy metabolism. We first tried to identify factors secreted by adipocytes in response to IL-13 and IL-4 and then examined their local and systemic effects. We found that recombinant IL-4 and IL-13 induce adipose tissue and adipocytes to secrete GDF15 (both in vitro and in vivo) via the Janus kinase-activated (JAK)-STAT6 pathway. Systemic increases in GDF15 levels in response to recombinant IL-13 were associated with improved glucose utilization by mice fed an HFD; however, these effects were not observed in GDF15 KO mice fed the HFD. We therefore propose that the beneficial effects of Th2 cytokines with respect to systemic glucose metabolism and insulin sensitivity are mediated by GDF15.

RESEARCH DESIGN AND METHODS

Mice and Ethical Considerations

STAT6 KO mice and their wild-type (WT) littermates (all with BALB/c background) were purchased from The Jackson Laboratory (Bar Harbor, ME). GDF15 KO mice derived from the inbred C57BL/6 strain were provided by Dr. S. Lee (Johns Hopkins University School of Medicine, Baltimore, MD). All in vivo experiments were conducted on male mice to avoid any effects of estrogen on Th2 cytokine production (14,15). All mice derived from the inbred C57BL/6 strain were housed in a specific pathogen-free animal facility (Chungnam National University Hospital Preclinical Research Center) in a controlled environment (12 h light/12 h dark cycle; humidity, 50–60%; ambient temperature, 22° ± 2°C) and fed a normal chow diet or an HFD that contained 60% fat (D12492; Research Diets Inc., New Brunswick, NJ). All animals received humane care according to institutional guidelines, and the Chungnam National University School of Medicine Institutional Review Board approved all experimental procedures.

Cell Culture

3T3-L1 cells were purchased from the American Type Culture Collection (Manassas, VA) and maintained in DMEM (Hyclone, Logan, UT) supplemented with 10% newborn calf serum (Gibco, Grand Island, NY) and 1% penicillin/streptomycin (Gibco) in a humidified incubator containing 5% CO_2. After 48 h, cells were differentiated by exposure to 3-isobutyl-1-methylxanthine (0.5 mmol/L), dexamethasone (1 μmol/L), insulin (10 μg/mL), and 10% FBS. Adipose-derived stem cells (ADSCs) were cultured as previously described (16) and differentiated into adipocytes by culture in M199 medium (Sigma-Aldrich, St. Louis, MO) supplemented with 10% FBS, 3-isobutyl-1-methylxanthine (0.5 mmol/L), dexamethasone (1 μmol/L), insulin (10 μg/mL), and rosiglitazone (0.5 mmol/L). Purified recombinant mouse IL-13 (413-ML) and recombinant mouse IL-4 (404-ML) used for the in vitro experiments were purchased from R&D Systems (Minneapolis, MN). Recombinant mouse IL-13 (210-13) and recombinant mouse IL-4 (214-14) used for the in vivo experiments were purchased from PeproTech (Rocky Hill, NJ).

Western Blot Analysis

3T3-L1 adipocytes, adipose tissue, and mouse liver were lysed in radioimmunoprecipitation assay buffer (30 mmol/L Tris [pH 7.5], 150 mmol/L sodium chloride, 1 mmol/L phenylmethylsulfonyl fluoride, 1 mmol/L sodium orthovanadate, 1% Nonidet P-40, 10% glycerol, and phosphatase and protease inhibitors). Western blot analysis of protein (30–50 μg) was performed according to standard procedures using the following commercially available antibodies: anti-STAT6, anti-phosphorylated (p)STAT6, anti-STAT3, and anti-pSTAT3 (Cell Signaling Technology, Beverley, MA). Appropriate secondary antibodies were obtained from Santa Cruz Biotechnology (Dallas, TX). Images were scanned using the Odyssey imaging system and quantified using Image Studio Digits (LI-COR Biosciences, Lincoln, NE).

RNA Sequencing Analysis

Total RNA was prepared from 3T3-L1 cells (treated with recombinant IL-13 or vehicle) using TRIzol reagent (Life Technologies), and poly(A) RNA was extracted using Dynabeads Oligo(dT)25 (Invitrogen). Sequencing libraries were prepared using Epicentre ScriptSeq v2, and 100 nucleotide paired-end sequencing was performed on an Illumina HiSeq2000 (Illumina Inc., San Diego, CA). The libraries were quantitated by quantitative (q)PCR in accordance with the qPCR Quantification Protocol Guide, and quality control was performed using an Agilent 2100 Bioanalyzer (Agilent Technology Inc., Santa Clara, CA). Reads were aligned with the *Mus musculus* genome build (mm10) using TopHat v2.0.13 (17). The reference genome and annotation data were downloaded from the University of California, Santa Cruz Genome Browser (http://genome.ucsc.edu). Gene annotation information was used to run TopHat using the "-G" option. After aligning the reads with the genome, we used Cufflinks v2.2.1 to assemble aligned reads into transcripts and estimate their abundance (18). The "–mas-bundle-frags 50000000" option was used to correct sequence expression count bias. The transcript counts at the isoform level were calculated, and relative transcript abundances were measured as FPKM (fragments per kilobase of exon

per million fragments mapped) using Cufflinks, along with gene expression values. FPKM values for each gene were calculated using Cufflinks v2.2.1, and the GENCODE v.24 general transfer format file was downloaded from the Human Genome Browser at the University of California, Santa Cruz. FPKM values ≤0 were excluded from further analysis. To facilitate $\log_2$ transformation, 1 was added to each FPKM value for the filtered genes. Filtered data were $\log_2$-transformed and subjected to quantile normalization. The resulting values were used for differentially expressed gene analysis. A fold change of two or more was deemed significant.

Plasmid Construction and Site-Directed Mutagenesis

pCMV-STAT6 was purchased from Addgene (Cambridge, MA). The pGL3B-human *GDF15* (−1,739/+70) luciferase reporter constructs were provided by Dr. Y. Moon (Pusan National University, Pusan, Korea). The pGL3B-*GDF15* deletion (STAT6 RE [−660 base pair]) plasmid was constructed by inserting the PCR-amplified fragment of the human GDF15 promotor into the *Kpn*I/*Xho*I-digested pGL3Basic vector (Promega Corp., Madison, WI). The nucleotide sequence of the 5′-flanking region of the GDF15 promoter was scanned, and one putative STAT6-binding site (−670 to −661, TTCCTGGAA) was identified. To create a STAT6 mutRE point-mutant reporter (GDF15 STAT6mut-Luc [−1,739/+70]), the 5′-gaagacTTCCTGGAAgaggggctttttgcg-3′ sequence of the STAT6 RE (−670) vector was mutated to 5′gaagacCCCAACCCCgaggggctttttgcg-3′ using DpnI-based site-directed mutagenesis (Agilent Technologies). The nucleotide sequences of all plasmids were confirmed by automated sequencing.

Luciferase Assay

3T3-L1 cells were plated in 12-well culture plates and transfected with the pCMV-STAT6 vector (1 μg), the human GDF15 (−1,739/+70) promoter luciferase reporter (100 ng), and a *Renilla* reporter vector (30 ng), along with the indicated expression plasmids (100–300 ng), using Lipofectamine PLUS (Invitrogen). An empty pcDNA3.1 vector was also added to ensure that the same total amount of plasmid DNA was used for each transfection. Next, transfected cells were treated with recombinant mouse IL-13 (100 ng/mL) or IL-4 (100 ng/mL). After 24 h, cells were lysed and luciferase assays were performed using a luciferase assay kit (Promega). The transfection efficiency was normalized against *Renilla* luciferase activity. All assays were performed at least in triplicate.

Small Interfering RNA Targeting IL-4 Receptor-α and Transfection of 3T3L1 Cells

Mouse IL-4 receptor-α (*Il4ra*) small interfering (si)RNA was obtained from Thermo Fisher Scientific (Waltham, MA). 3T3L1 cells were seeded into 12-well plates transfected (on day 1) with *Il4ra* small interfering (si) RNA or negative scramble siRNA Lipofectamine PLUS. The transfected cells were incubated in medium containing 10% FBS and then treated with recombinant IL-4 or IL-13 for 24 h. Finally, the cells and supernatants were used for analysis of STAT6 signaling and GDF15.

Stimulation of Murine Invariant Natural Killer T Cells

WT C57BL/6 mice received an intraperitoneal injection of 2 μg (87 μg/kg) of α-galactosylceramide (αGC) [(2S,3S,4R)-1-*O*-(α-*d*-galactopyranosyl)-2-(N-hexacosanoylamino)-1,3,4-octadecanetriol] or saline alone. The mice were sacrificed 4 days later before further analysis (19). IL-4 (R&D Systems), IL-13 (R&D Systems), GDF15 (R&D Systems), and interferon-γ (IFN-γ; eBioscience) were measured in the serum using ELSIA kits obtained from the indicated suppliers. Adipose-derived stromal vascular cells (SVCs) were isolated and analyzed by flow cytometry.

Isolation of Adipocytes and SVCs

Adipose tissues were isolated from mice and minced into fine pieces with sterile scissors. Minced samples were placed in HEPES-buffered PBS containing 10 mg/mL BSA (Sigma-Aldrich) and type 1 collagenase (1 mg/mL; Worthington Biochemical Corp., Lakewood, NJ) at 37°C and incubated on an orbital shaker for 30 min, followed by centrifugation at 1,000*g* for 5 min at 4°C to remove erythrocytes and other blood cells. Once digestion was complete, samples were passed through a sterile 70-μm cell strainer (BD Falcon, Franklin Lakes, NJ). The suspension was then centrifuged at 1,000*g* at 4°C for 5 min, and the pellet was collected (designated SVCs). The floating cells were collected and designated as the adipocyte-enriched fraction. SVCs were gently resuspended in Red Blood Cell Lysis Buffer (Sigma-Aldrich) and incubated at 24°C for 5 min. The red blood cell–depleted SVCs were the recentrifuged at 500*g* for 5 min, and the pellet was frozen in liquid nitrogen.

Recombinant IL-33–Mediated Activation of Th2 Cytokines

Mice (8 weeks old) received an intraperitoneal injection of vehicle or recombinant mouse IL-33 (0.5 μg per mouse [22 μg/kg]); BioLegend, San Diego, CA) once daily for 8 days (20). To investigate the pharmacological effect of IL-13 on whole-body glucose homeostasis, 8-week-old WT C57BL/6J or GDF15 KO mice were fed an HFD or normal chow diet for 8 weeks. After 6 weeks, the mice received intraperitoneal injections of recombinant mouse IL-13 (0.5 μg per mouse [22 μg/kg]) or PBS alone (once daily for 10 days). At the conclusion of the experiments, adipose and liver tissues were harvested and snap frozen in liquid nitrogen before molecular analyses and were fixed in 10% formalin for histological analyses or digested with type 1 collagenase before flow cytometric analyses of adipose immune cells.

Glucose and Insulin Tolerance Tests

Mice were fasted for 16 h before the glucose tolerance test. Next, glucose (2 g/kg of body weight) was injected into the intraperitoneal cavity, and blood glucose and insulin levels were measured with a glucometer (Accu-Chek Active; Roche Diagnostics, Indianapolis, IN) at 0, 15, 30, 60, 90, and 120 min. For the insulin tolerance test, mice were fasted for 6 h before receiving an intraperitoneal injection of insulin

(0.75 units/kg; Humalog; Eli Lilly, Indianapolis, IN), and blood glucose levels were measured at 15, 30, 60, 90, and 120 min.

FACS Analyses

Adipose tissues were excised and minced in collagenase buffer. The minced tissues were digested with type 1 collagenase for 40 min at 37°C with gentle shaking and then filtered through a 100-μm filter. Digested cells were obtained by centrifugation at 800*g* for 5 min and incubated with Red Blood Cell Lysis Buffer. To identify eosinophils and M1 and M2 macrophages, SVCs were stained with the Live/Dead marker 7AAD (BD Biosciences, San Jose, CA), followed by anti-CD45, anti-CD11b, anti-F4/80, and anti–Siglec-F antibodies (all from BioLegend). To detect intracellular CD206, stained cells were fixed and permeabilized with Cytofix/Cytoperm (BD Biosciences), followed by an anti-CD206 antibody. The gating strategy used to analyze M1/M2 polarization is described in Supplementary Fig. 9. To identify CD4 T cells, CD8 T cells, and B cells, SVCs were stained with the Live/Dead marker 7AAD, followed by anti-CD45, anti-CD3, anti-CD4, anti-CD8, and anti-B220 antibodies (all from BioLegend). The stained cells were analyzed using a FACS Canto II flow cytometer (BD Biosciences), and data were analyzed using FlowJo software (FlowJo, LLC, Ashland, OR).

Statistical Analysis

Statistical analyses were performed using GraphPad Prism 6 (GraphPad Software Inc., La Jolla, CA). Data are reported as the mean ± SD. All data from animal studies were analyzed by two-way repeated-measures ANOVA, followed by Bonferroni multiple comparisons, one-way ANOVA followed by the Tukey post hoc test, or a two-tailed Student *t* test. *P* values <0.05 were considered statistically significant.

RESULTS

Th2 Cytokines, IL-13 and IL-4, Activate the JAK-STAT6 Pathway in Adipocytes

A recent study shows that Th2 cytokines ameliorate chronic inflammation in adipose tissue by activating the STAT6 pathway (11). The action of Th2 cytokines in cells and tissues is mediated by heterodimerization of IL-13Rα and IL-4Rα to form a receptor complex that binds IL-13 and IL-4, thereby activating the JAK/STAT6 pathway (21,22). Although Th2 cytokines also upregulate expression of their own receptors expressed by murine immune cells, including T and B cells, and by human keratinocytes (23–25), whether this is the case in adipocytes is not known. Therefore, we first examined the effect of IL-13 and IL-4 on the expression of their cognate receptors on 3T3-L1 adipocytes. Compared with vehicle treatment, expression of *Il13ra1* by adipocytes markedly increased after treatment with recombinant IL-13 and/or IL-4 (Fig. 1*A*). Recombinant IL-13 was a more potent inducer of *Il13ra1* than recombinant IL-4 (Fig. 1*A*). *Il4ra1* expression by Th2 cytokine–treated 3T3-L1 adipocytes also increased, but the difference between treatment with recombinant IL-13 or IL-4 was not significant (Fig. 1*B*). Phosphorylation of STAT6 in 3T3-L1 adipocytes exposed to recombinant IL-13 or IL-4 also increased (Fig. 1*C* and *D*) in various time points (Fig. 1*E* and *F*). STAT6 phosphorylation in differentiated 3T3-L1 adipocytes also occurred after treatment with recombinant IL-13 or IL-4 (Fig. 1*G* and *H*). Moreover, treatment with Th2 cytokines increased STAT6 phosphorylation in differentiated ADSCs (Fig. 1*I*). Finally, a broad spectrum JAK inhibitor (JAK I) reduced Th2 cytokine–mediated phosphorylation of STAT6 in 3T3-L1 adipocytes (Fig. 1*J*). Previous studies show that Th2 cytokines induce STAT3 phosphorylation in a variety of cell types (26,27). Thus, we checked whether Th2 cytokines affect STAT3 phosphorylation in undifferentiated and differentiated 3T3-L1 adipocytes as well as in ADSCs. We found that Th2 cytokines had no significant effect on STAT3 in adipocytes (Supplementary Fig. 1*A*–*G*). However, STAT3 phosphorylation in 3T3-L1 adipocytes decreased in the presence of JAK I (Supplementary Fig. 1*H*). Collectively, these data suggest that Th2 cytokines activate the JAK1-STAT6 pathway but not the STAT3 pathway in different types of adipocytes.

Th2 Cytokines Induce GDF15 Production by Adipocytes

To identify the gene sets regulated by IL-13–mediated activation of the STAT6 pathway in 3T3-L1 adipocytes, we performed transcriptome analysis using RNA sequencing (18). Compared with control cells, we identified 115 genes that were upregulated by at least twofold and 71 genes that were downregulated by at least twofold in 3T3-L1 adipocytes treated with recombinant IL-13 (Fig. 2*A*). We analyzed the gene expression data obtained by RNA sequencing and found that six representative Gene Ontology Biological Process terms were enriched in 3T3-L1 adipocytes treated with recombinant IL-13 (Supplementary Fig. 2*A*). Gene set enrichment analysis revealed a strong correlation between genes upregulated in 3T3-L1 adipocytes treated with recombinant IL-13 and a gene set linked to inflammatory responses (Fig. 2*B* and Supplementary Fig. 2*B*). Genes related to the JAK-STAT signaling pathway, cytokine-cytokine receptor interactions, and chemokine signaling pathways were also upregulated in 3T3-L1 adipocytes treated with recombinant IL-13 (Fig. 2*C* and Supplementary Fig. 2*C*–*F*). Analysis of heat maps and volcano plots revealed that expression of multiple secretory factors was significantly higher in 3T3-L1 adipocytes treated with recombinant IL-13 than in controls (Fig. 2*D* and *E*). Real-time PCR analysis revealed that treatment with recombinant IL-13 also increased expression of secretory factors in 3T3-L1 adipocytes (Fig. 2*F*). In line with previous studies (28,29), we found that genes involved in chemoattraction of eosinophils, such as *Ccl11* and *Ccl7*, were upregulated in 3T3-L1 adipocytes treated with Th2 cytokines. Expression of *Il6* and *Ccl2* also increased in 3T3-L1 adipocytes treated with recombinant IL-13, a phenomenon that may be associated with activation of JAK-STAT signaling (30). Although in vitro treatment of cultured cells with recombinant IL-13 increased

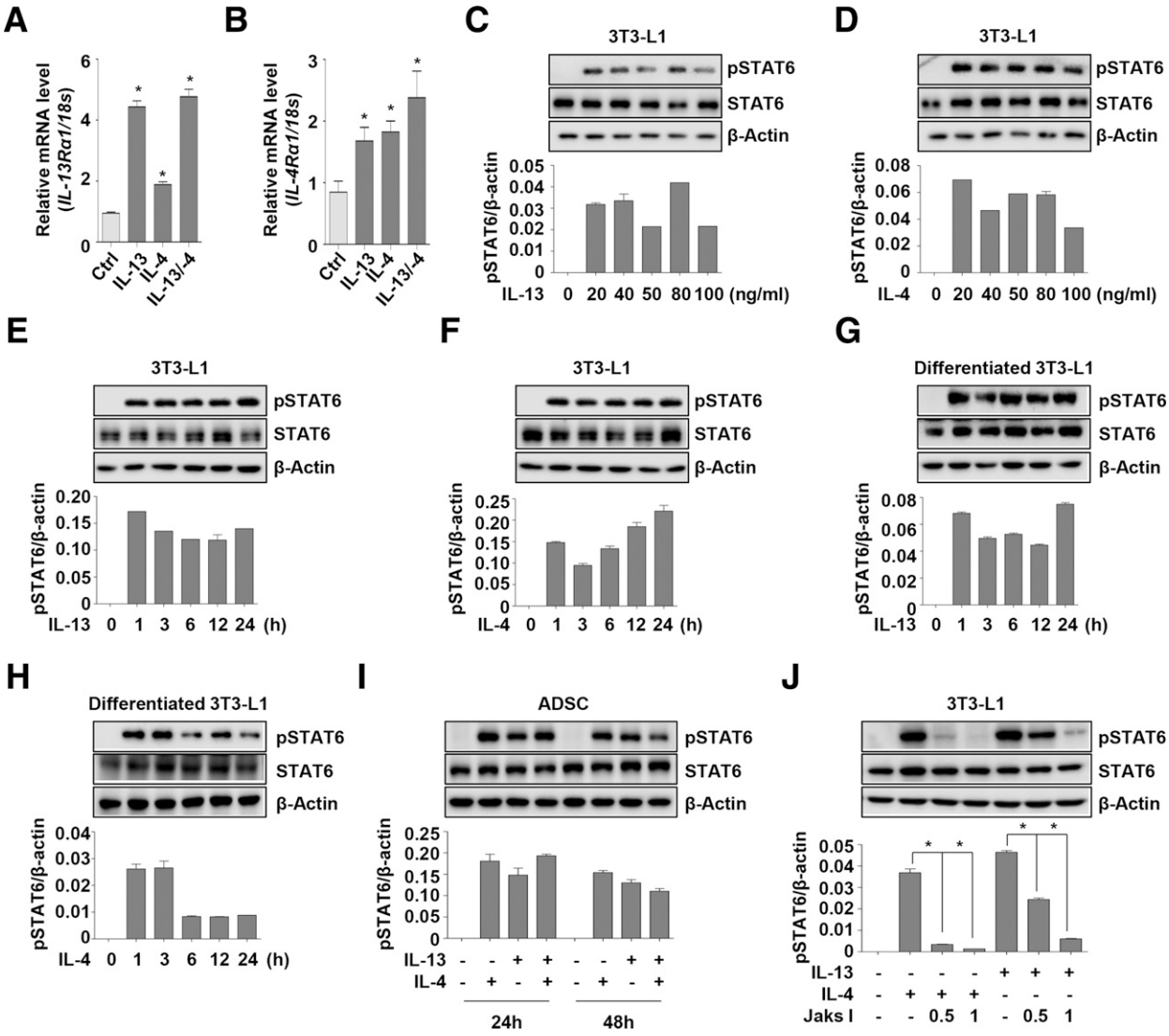

Figure 1—Th2 cytokines increase STAT6 phosphorylation in cultured adipocytes and ADSCs. *A* and *B*: Real-time PCR analysis of 3T3-L1 adipocytes treated with recombinant IL-4, IL-13, or control (Ctrl) vehicle. *C* and *D*: Western blot analysis of pSTAT6 and STAT6 expression by 3T3-L1 adipocytes treated with various concentrations of recombinant IL-4 or IL-13 (0, 20, 40, 50, 80, and 100 ng/mL) or with vehicle alone. *E* and *F*: Western blot analysis of pSTAT6 and STAT6 expression by 3T3-L1 adipocytes treated with recombinant IL-13 or IL-4 (100 ng/mL) or with vehicle alone for 0 to 24 h. *G* and *H*: Western blot analysis of pSTAT6 and STAT6 expression by differentiated 3T3-L1 adipocytes treated with recombinant IL-4 or IL-13 or with vehicle alone for 0 to 24 h. *I*: Western blot analysis of pSTAT6 and STAT6 expression by ADSCs treated with recombinant IL-13, IL-4, or with vehicle alone for 24 and 48 h. *J*: Western blot analysis of pSTAT6 and STAT6 expression by 3T3-L1 adipocytes treated with vehicle, recombinant IL-4, IL-13, and/or JAK inhibitors. *C*–*J*: Densitometry was used for relative quantification of each protein. All data are representative of three independent experiments and are expressed as the mean ± SEM. **P* < 0.05 vs. the corresponding controls.

expression of genes related to inflammation, we did not find a significant increase in serum levels of IFN-γ in mice treated with IL-13 (Supplementary Fig. 2*G*) compared with controls. This indicates that IL-13–stimulated expression of inflammatory genes might not be crucial for systemic glucose homeostasis by IL-13.

Th2 cytokines are also involved in reconstituting M2 polarized macrophages in adipose tissue, leading to improved insulin sensitivity and glucose homeostasis (1). Among the secretory factors induced by recombinant IL-13, GDF15 ameliorates glucose intolerance and insulin resistance in mice (31,32). Therefore, we next examined the effect of Th2 cytokines on GDF15 secretion by cultured adipocytes. As shown in Fig. 2*G* and Supplementary Fig. 3*A*, recombinant IL-13 increased the level of GDF15 in supernatants from cultured ADSCs and 3T3-L1 adipocytes. Treatment with recombinant IL-4 also increased the expression of *Gdf15* by 3T3-L1 adipocytes as well as the GDF15 concentration in supernatants from both cultured 3T3-L1 adipocytes and ADSCs (Fig. 2*H* and Supplementary Fig. 3*B* and *C*). Moreover, treatment with Th2 cytokines increased the GDF15 concentration in supernatants from differentiated ADSCs (Fig. 2*I* and *J*). We found that recombinant IL-4 and IL-13 increased secretion of GDF15 by primary

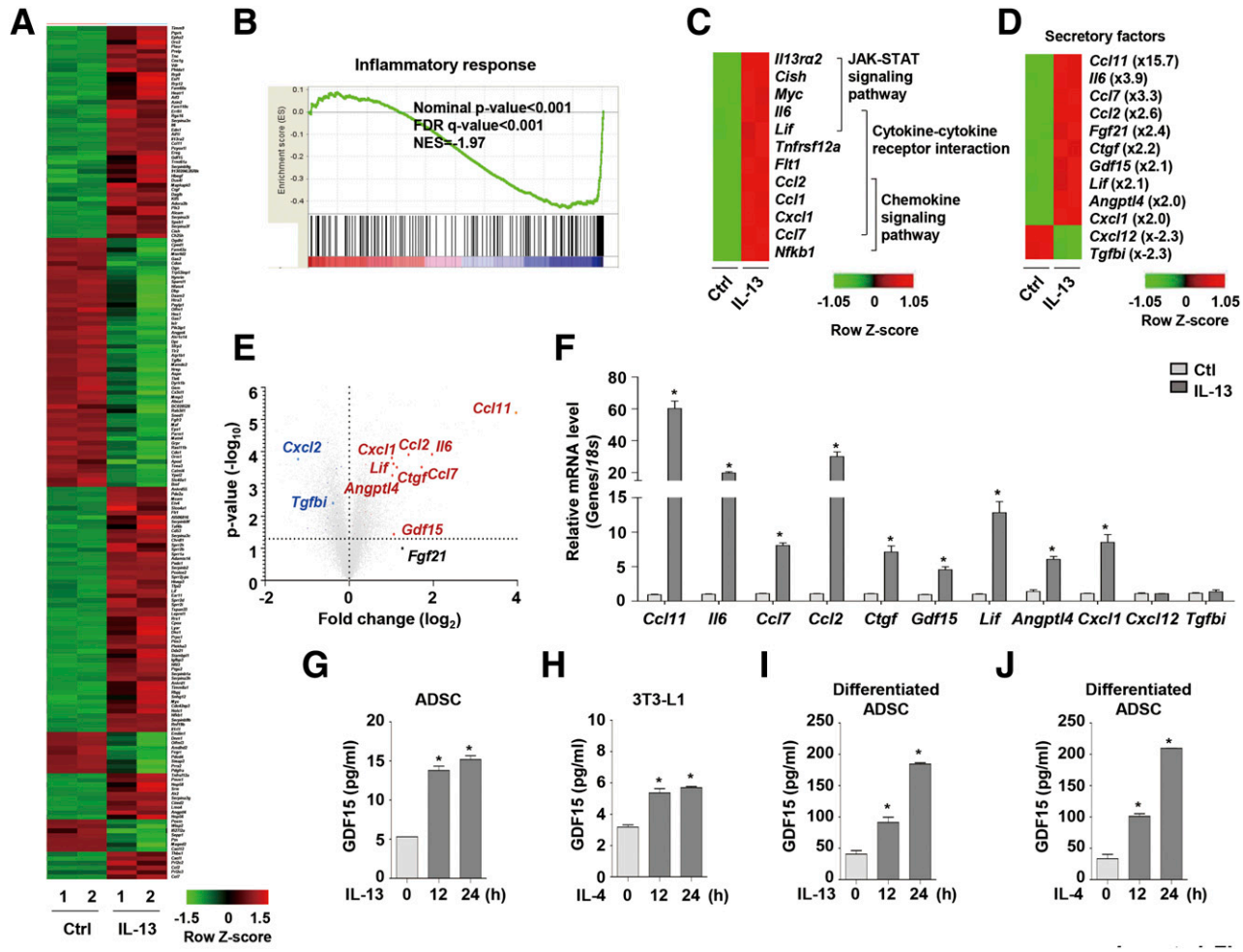

Figure 2—IL-13 induces GDF15 expression by cultured adipocytes and ADSCs. *A*: Heat map of genes differentially expressed in 3T3-L1 adipocytes treated with recombinant IL-13 (100 ng/mL) (twofold or more change in expression compared with control [Ctrl] vehicle). *B*: The diagram shows the result of Gene Set Enrichment Analysis, including the normalized enrichment scores (NES). FDR, false discovery rate. *C* and *D*: Heat map of differential expression of genes associated with signaling pathways and secretory factors in 3T3-L1 adipocytes treated with recombinant IL-13 (100 ng/mL) compared with vehicle. *E*: Volcano plot showing differential expression, and the significance of the differences, of 24,067 Affymetrix gene probes. The red (upregulated) or blue (downregulated) dots represent genes associated with $P < 0.05$ and a −fold change >1 $\log_2$. *F*: 3T3-L1 adipocytes treated with recombinant IL-13 (100 ng/mL) or vehicle were analyzed with real-time PCR. *G*: GDF15 levels in supernatants from ADSCs treated with recombinant IL-13 (100 ng/mL) for 12 or 24 h. *H*: GDF15 levels in supernatants from 3T3-L1 adipocytes treated with recombinant IL-4 (100 ng/mL) for 12 or 24 h. *I* and *J*: GDF15 levels in supernatants from differentiated ADSCs treated with recombinant IL-13 or IL-4 (100 ng/mL) for 12 or 24 h. Data are expressed as the mean ± SEM. *$P < 0.05$ compared with the corresponding controls.

hepatocytes and C2C12 myotubes in vitro (Supplementary Fig. 3*D*–*G*).

STAT6 Is Necessary for Th2 Cytokine–Mediated GDF15 Production by Adipocytes

Based on our observation that Th2 cytokines drive expression of GDF15, we next explored the role played by STAT6 during GDF15 expression by cultured adipocytes. Overexpression of STAT6 by 3T3-L1 adipocytes induced *GDF15* promotor activity (Fig. 3*A* and *B*). The amount of GDF15 protein in the supernatants from cultured adipocytes was increased significantly in the presence of vehicle or a STAT6 overexpression vector in response to Th2 cytokines (Fig. 3*C*). To confirm that the GDF15 promoter harbors STAT6-responsive elements, we scanned the nucleotide sequence of the 5′-flanking region of the *GDF15* promoter and identified one putative STAT6-binding site. We therefore created 3T3-L1 adipocytes harboring reporter plasmids carrying STAT6 deletion mutations or point mutations in the human *GDF15* promoter (Fig. 3*D* and Supplementary Fig. 4*A*). A luciferase reporter assay revealed the functional importance of putative STAT6-responsive elements within the human *GDF15* promoter in cultured adipocytes (Fig. 3*E* and Supplementary Fig. 4*B*). Unlike STAT6, overexpression of STAT1 or STAT3 did not increase GDF15 promoter activity in adipocytes (Supplementary Fig. 4*C*). Next, we showed that induction of *Gdf15* transcripts in 3T3-L1 adipocytes treated with IL-4 or IL-13 was inhibited by a JAK inhibitor (Fig. 3*F*). Furthermore, siRNA-mediated knockdown of IL4RA in cultured adipocytes abrogated IL-4– or IL-13–mediated STAT6 phosphorylation and expression

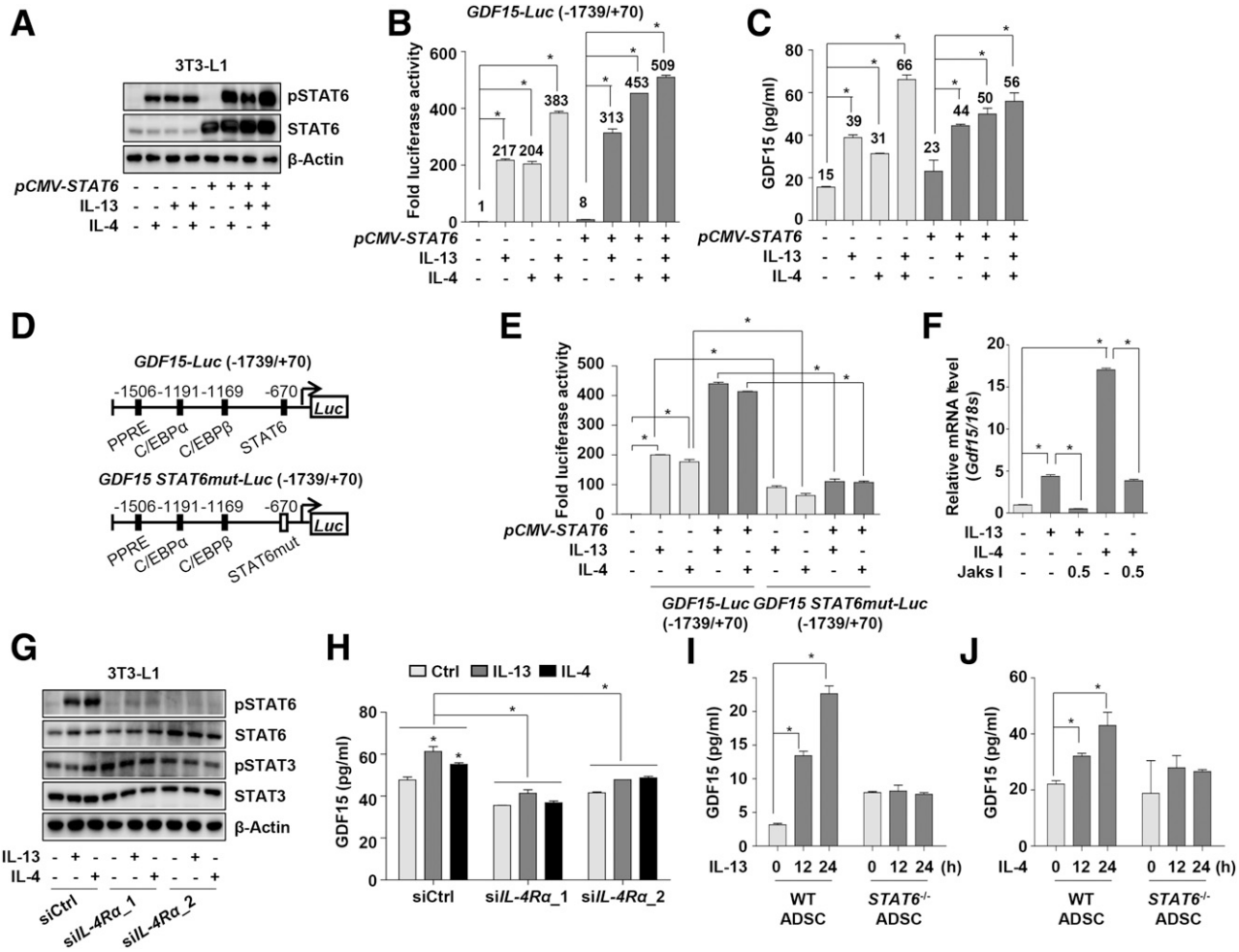

Figure 3—STAT6 is essential for Th2 cytokine-induced GDF15 expression by cultured adipocytes and ADSCs. *A*: Western blot analysis of pSTAT6 and STAT6 expression by 3T3-L1 cells exposed to vehicle, recombinant IL-4 (100 ng/mL), recombinant IL-13 (100 ng/mL), and/or *pCMV-STAT6* overexpression. *B*: *GDF15* promoter activity in 3T3-L1 cells induced by recombinant IL-13 and IL-4 and/or *pCMV-STAT6* overexpression. *C*: Amount of GDF15 protein in the supernatant from 3T3-L1 cells exposed to recombinant IL-13 (100 ng/mL), recombinant IL-4 (100 ng/mL), and/or *pCMV-STAT6* overexpression. *D*: Response element of the GDF15 luciferase (Luc) reporter (−1,739/+70) and point mutations (mut) in the human GDF15 promoter. *E*: Luciferase reporter activity of the GDF15 promoter and STAT6-mutated (mut) GDF15 promoter upon exposure to recombinant IL-13, recombinant IL-4, and or *pCMV-STAT6* overexpression. *F*: Level of *Gdf15* mRNA induced in 3T3-L1 cells by recombinant IL-13, recombinant IL-4, or JAK I. *G*: Western blot analysis of 3T3-L1 cells after addition of siRNA targeting IL-4Rα. Ctrl, control. *H*: Levels of GDF15 in supernatants from 3T3-L1 cells after addition of IL-4Rα siRNA. *I* and *J*: Amount of GDF15 protein in the supernatant from WT or STAT6 KO ADSCs treated with recombinant IL-13 or recombinant IL-4 for 12 h or 24 h. All data are representative of more than three independent experiments and are expressed as the mean ± SEM. **P* < 0.05 compared with the corresponding controls.

of GDF15 (Fig. 3*G* and *H*). Furthermore, we also observed Th2 cytokine induced production of GDF15 production by WT ADSCs but not by STAT6 KO ADSCs (Fig. 3*I* and *J*). These observations suggest that the IL4RA-STAT6 signaling axis mediates Th2 cytokine–induced GDF15 expression in adipocytes.

αGC Induces Production of GDF15 via the STAT6 Pathway in Adipose Tissue and Liver

Previous studies show that αGC increases the expression of Th2 cytokines by activating invariant natural killer T (iNKT) cells, which are enriched in adipose tissues and associated with reduced tissue inflammation and insulin resistance in mice (33). Therefore, we next asked whether αGC-induced iNKT cell activation promotes Th2 cytokine–mediated GDF15 production in mice. WT mice were treated with αGC to increase activation of iNKT cells; this is because iNKT cell–induced Th2 cytokines might contribute to the increase in GDF15 production in adipocytes. Treatment with αGC increased the absolute number of eosinophils in adipose tissue (Fig. 4*A*). Expression of IL-13 receptor-α 1 (IL13RA1) by adipocytes was also increased by αGC (Fig. 4*B*). Moreover, serum levels of Th2 cytokines, including IL-4 and IL-13, increased in mice treated with αGC (Fig. 4*C* and *D*), although αGC also increased serum IFN-γ levels as well as expression of *CD1d* in the WAT and liver (Supplementary Fig. 5*A* and *B*). Consistent with the increase in Th2 cytokine levels, αGC also increased GDF15 levels in

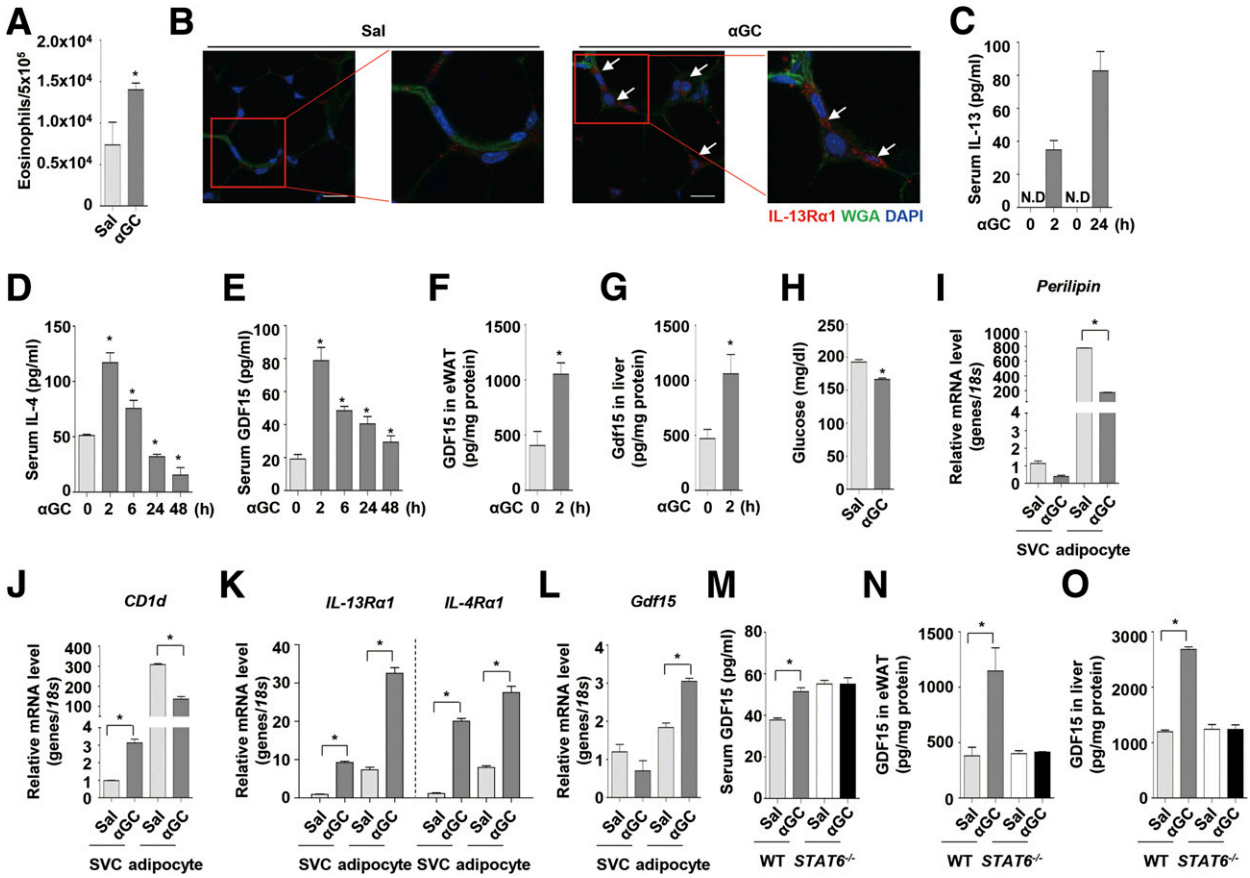

Figure 4—αGC increases STAT6-mediated GDF15 expression in adipose tissue and liver. *A*: Eosinophil ($CD45^+CD11b^+SiglecF^+$) population in eWAT from 10-week-old mice injected with saline (Sal) or αGC (n = 4 per group). *B*: Localization of IL-13Rα in eWAT of saline- or αGC-injected mice. IL-13Rα (red), wheat germ agglutinin (WGA) (green), and DAPI (blue) are shown. Arrows indicate IL-13Rα1 positivity. Scale bar, 20 μm. *C–E*: Levels of IL-13 (from 0 to 24 h) and IL-4 and GDF15 (from 0 to 48 h) in serum from αGC-injected mice. N.D., not detectable. *F* and *G*: GDF15 protein in eWAT and liver from mice exposed to αGC for 2 h. *H*: Random glucose levels in serum from saline- or αGC-injected mice (n = 4 per group). *I–L*: Expression of *Perilipin*, *CD1d*, *IL-13Rα1* and *IL-4Rα1*, and *Gdf15* mRNA in SVCs or adipocytes isolated from saline- or αGC-injected mice. *M–O*: GDF15 protein levels in the serum, eWAT, and liver from saline- or αGC-treated WT or STAT6 KO mice. Results are representative of three independent experiments and are expressed as the mean ± SEM. $^*P < 0.05$ compared with the corresponding controls.

serum (Fig. 4*E*). GDF15 expression in epididymal WAT (eWAT) and liver tissues also increased (Fig. 4*F* and *G* and Supplementary Fig. 5*C*). We also found it interesting that serum glucose levels fell in mice treated with αGC (Fig. 4*H*). However, expression of GDF15 was not increased in primary hepatocytes and C2C12 myotubes treated with αGC (Supplementary Fig. 5*D* and *E*). This indicates that αGC does not stimulate GDF15 expression in hepatocytes and myocytes directly. Taken together, these data suggest that αGC increases expression of both Th2 cytokines and GDF15 in mice.

To examine cell type–specific gene expression in adipose tissues, we collected eWAT depots from WT mice treated with or without αGC. These depots were then digested with type 1 collagenase and centrifuged to yield a buoyant adipocyte-enriched cell population and a pellet of SVCs. Although we found no significant difference in *Perilipin* and *Pparg* expression in SVCs from treated and nontreated mice, the expression in adipocytes was downregulated in mice injected with αGC (Fig. 4*I* and Supplementary Fig. 5*F*). This means that αGC reduced lipid storage in adipose tissue by downregulating *Perilipin* and *Pparg* expression. As expected, expression of *CD1d* was higher in SVCs from mice injected with αGC (Fig. 4*J*). Also, expression of *Il13ra1* and *Il4ra1* in the adipocyte fraction and SVCs was increased after treatment with αGC (Fig. 4*K*). However, *Gdf15* transcription was increased only in the adipocyte fraction (Fig. 4*L*), suggesting that αGC-induced Th2 cytokines promote *Gdf15* expression in adipocytes but not in adipose-infiltrating immune cells. In contrast to that in WT mice, αGC failed to increase serum levels of GDF15 in STAT6 KO mice (Fig. 4*M*). αGC-induced expression of GDF15 was also abolished in eWAT and liver tissues from STAT6 KO mice (Fig. 4*N* and *O*).

IL-33–Mediated Eosinophil Proliferation Increases GDF15 Production in Adipose Tissue via IL-13

To exclude the possibility that αGC has hepatotoxic effects that mediate production of GDF15 in mice, we used another mouse model to demonstrate Th2 cytokine–mediated

GDF15 expression. IL-33 activates ILC2, which in turn induces IL-5–mediated proliferation of eosinophils (34). Because proliferation and activation of eosinophils increases the serum levels of IL-4 and IL-13, we treated mice with recombinant IL-33 and examined whether Th2 cytokines induced by eosinophils increased GDF15 production in adipose tissues. As expected, recombinant IL-33 induced higher level of ILC2 and eosinophils in adipose tissues, with no evidence of hepatotoxicity (Fig. 5*A* and *B* and Supplementary Fig. 6*A* and *B*); however, we observed no IL-33–induced increase in the eosinophil population in STAT6 KO mice (Fig. 5*C*). Serum IL-13 levels in IL-33–treated mice were significantly higher than those in saline-treated mice (Fig. 5*D*). In accordance with increased IL-13 levels, GDF15 levels in serum and adipose tissue of WT mice injected with recombinant IL-33 also increased (Fig. 5*E* and *F*). By contrast, IL-33–mediated GDF15 production (local and systemic) was abolished in STAT6 KO mice (Fig. 5*E–G*). Moreover, serum levels of glucose in the mice treated with recombinant IL-33 were markedly lower than those in control mice, although food consumption and body weight did not differ significantly (Fig. 5*H* and Supplementary Fig. 6*C* and *D*). There was no difference in insulin levels in mice treated with saline or recombinant IL-33 (Fig. 5*I*). Expression of GDF15 by primary hepatocytes and C2C12 myotubes was not directly affected by recombinant IL-33 (Supplementary Fig. 6*E* and *F*). Taken together, these findings suggest that IL-33–mediated activation of Th2 cytokine–mediated STAT6 signaling contributes to GDF15 production in adipose tissue in mice, resulting in reduced serum glucose levels.

IL-13 Improves Glucose Tolerance via GDF15 Production

The data described above show that Th2 cytokines, particularly IL-13, induce GDF15 expression in cultured adipocytes and adipose tissue via the JAK-STAT6 pathway. Although previous studies show that GDF15 increases longevity and protects mice against obesity and insulin resistance (31,32,35), the effects of Th2 cytokine–mediated GDF15 production on glucose homeostasis and insulin sensitivity remain unclear. Therefore, to examine the effects of Th2 cytokine–mediated GDF15 production on weight gain and insulin resistance, we injected mice intraperitoneally daily with recombinant IL-13 or vehicle for 10 days, beginning at 8 weeks of age. Weight gain was lower and the expression of *Il13ra1* and *Il4ra1* was higher in the adipose tissue of IL-13–treated mice than in vehicle-treated controls (Fig. 6*A–C*), independent of food intake and liver damage (Fig. 6*D* and *E* and Supplementary Fig. 7*A*). As expected,

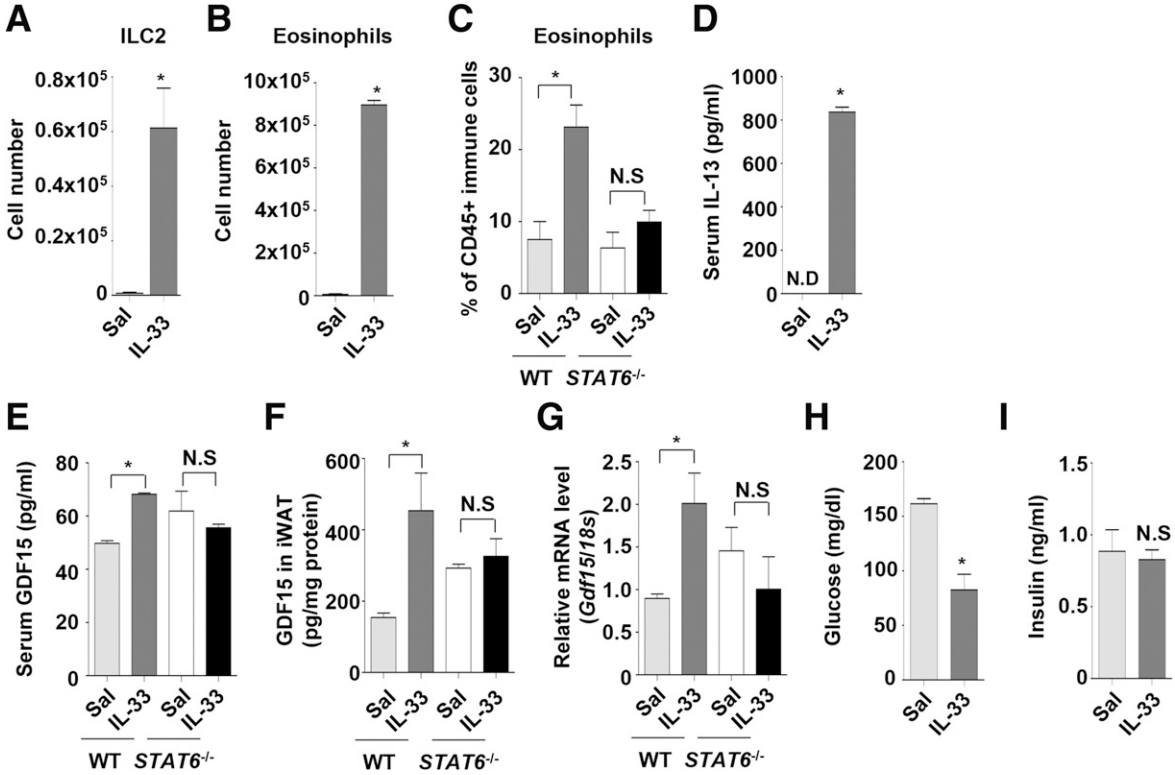

Figure 5—IL-33–mediated production of GDF15 in adipose tissue. *A–C*: Number of ILC2 ($Lin^-IL\text{-}7R\alpha^+ST2^+$) cells and number and percentage of eosinophils ($CD45^+CD11b^+SiglecF^+$) in eWAT from WT or STAT6 KO mice treated with recombinant IL-33 ($n = 5$ per group). Recombinant IL-33 (0.5 μg) was administered for 8 days by intraperitoneal injection. Sal, saline. *D*: Levels of IL-13 in serum from mice injected with recombinant IL-33. N.D., not detectable. *E–G*: Amount of GDF15 protein and transcripts in serum and inguinal WAT (iWAT) from WT or STAT6 KO mice treated with recombinant IL-33. *H* and *I*: Blood glucose and serum insulin levels of mice treated with saline or recombinant IL-33. Data are representative of three independent experiments and are expressed as the mean ± SEM. $^*P < 0.05$ compared with the corresponding controls.

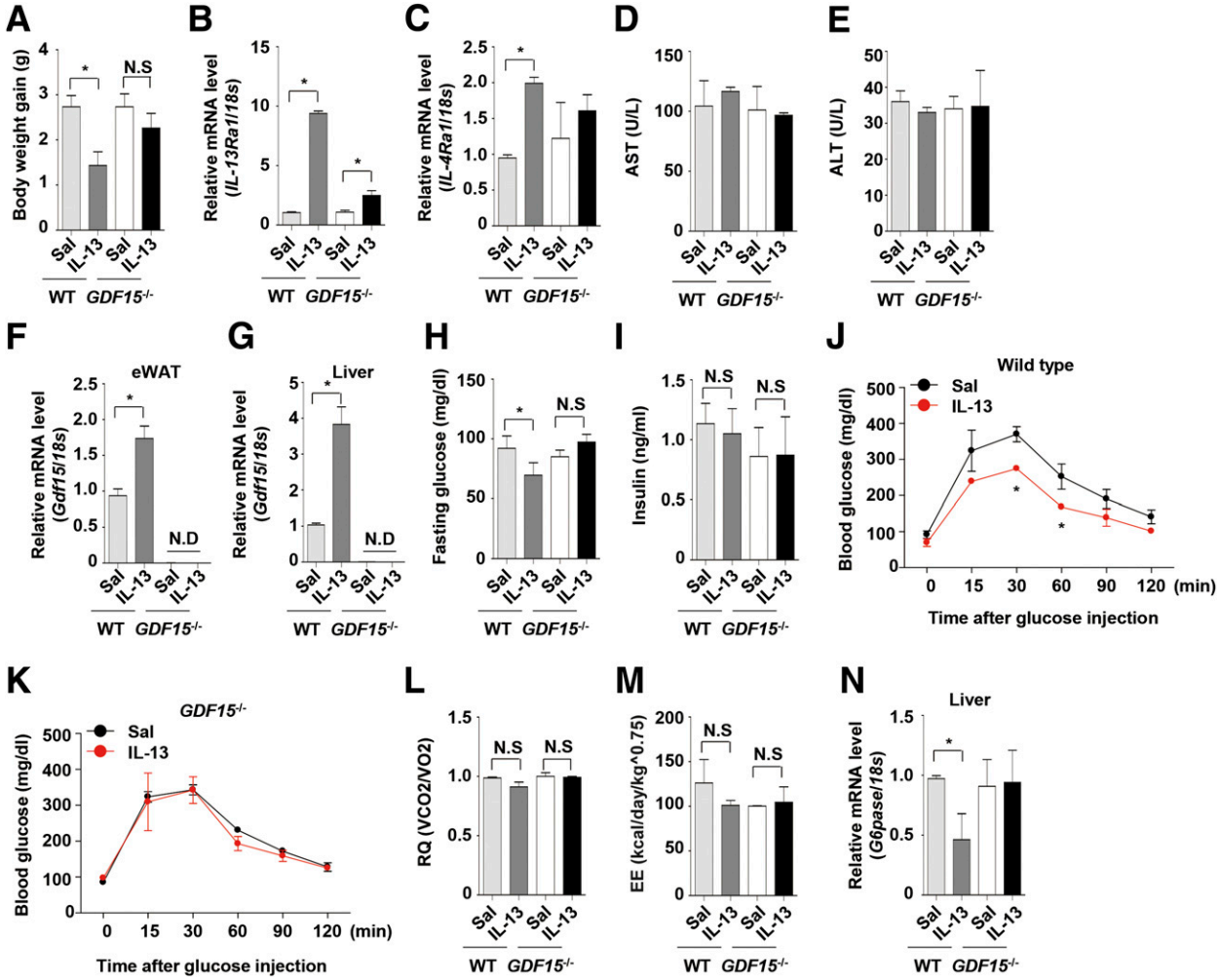

Figure 6—GDF15 is essential for Th2 cytokine–mediated glucose homeostasis. *A*: Body weight gain by WT or GDF15 KO mice treated with recombinant IL-13 (0.5 μg; $n = 5$ per group). *B* and *C*: Relative expression of *IL-13Rα1* and *IL-4Rα1* mRNA in eWAT from WT and GDF15 KO mice treated with saline or recombinant IL-13. *D* and *E*: Aspartate transaminase (AST) and alanine transaminase (ALT) levels in serum from mice treated with recombinant IL-13. *F* and *G*: Expression of adipose and hepatic *Gdf15* mRNA in WT and GDF15 KO mice treated with recombinant IL-13. *H* and *I*: Fasting glucose and serum insulin levels of WT and GDF15 KO mice treated with recombinant IL-13. *J* and *K*: Glucose tolerance test results for WT and GDF15 KO mice treated with recombinant IL-13. *L* and *M*: Respiratory quotient (RQ; VCO_2/VO_2) and energy expenditure (EE) by WT and GDF15 KO mice treated with recombinant IL-13. *N*: Expression of hepatic *G6pase* mRNA in WT and GDF15 KO mice treated with recombinant IL-13. All data are representative of three independent experiments and are expressed as the mean ± SEM. $^*P < 0.05$ compared with the corresponding controls. N.D., not detectable; Sal, saline.

expression of *Gdf15* in the adipose tissue and liver of mice treated with recombinant IL-4 or IL-13 was higher than in controls (Fig. 6*F* and *G* and Supplementary Fig. 7*B* and *C*). Serum levels of GDF15 and expression of *Gdf15* in muscle was also increased in mice treated with recombinant IL-4 or IL-13 (Supplementary Fig. 7*D* and *E*). The serum glucose in recombinant IL-13–treated mice was lower than that in vehicle-treated mice; however, this effect was abolished in GDF15 KO mice (Fig. 6*H*). Injection of recombinant IL-13 did not alter insulin levels in WT or GDF15 KO mice (Fig. 6*I*). Moreover, the glucose R_d in response to the intraperitoneal glucose challenge was higher in recombinant IL-13–treated mice than in control mice; this improved glucose tolerance was attenuated in GDF15 KO mice (Fig. 6*J* and *K*). However, IL-13 had no significant effect on VO_2, VCO_2, and energy expenditure (adjusted by body weight) in WT or GDF15 KO mice (Fig. 6*L* and *M*). Injection of recombinant IL-13 reduced expression of a key regulator of gluconeogenesis (*G6pase*) in WT mice but not in GDF15 KO mice (Fig. 6*N*).

GDF15 Is Required for IL-13–Induced Improvement of Glucose Intolerance in Mice Fed an HFD

Given that murine adipose tissue secretes high amounts of GDF15, we next investigated whether IL-13–mediated GDF15 expression protects WT and GDF15 KO mice against obesity and insulin resistance. Treatment of WT mice with recombinant IL-13 increased *Gdf15* transcription in the adipocyte-enriched fraction but not the SVC fraction from adipose tissues as well as in the liver (Fig. 7*A* and *B*).

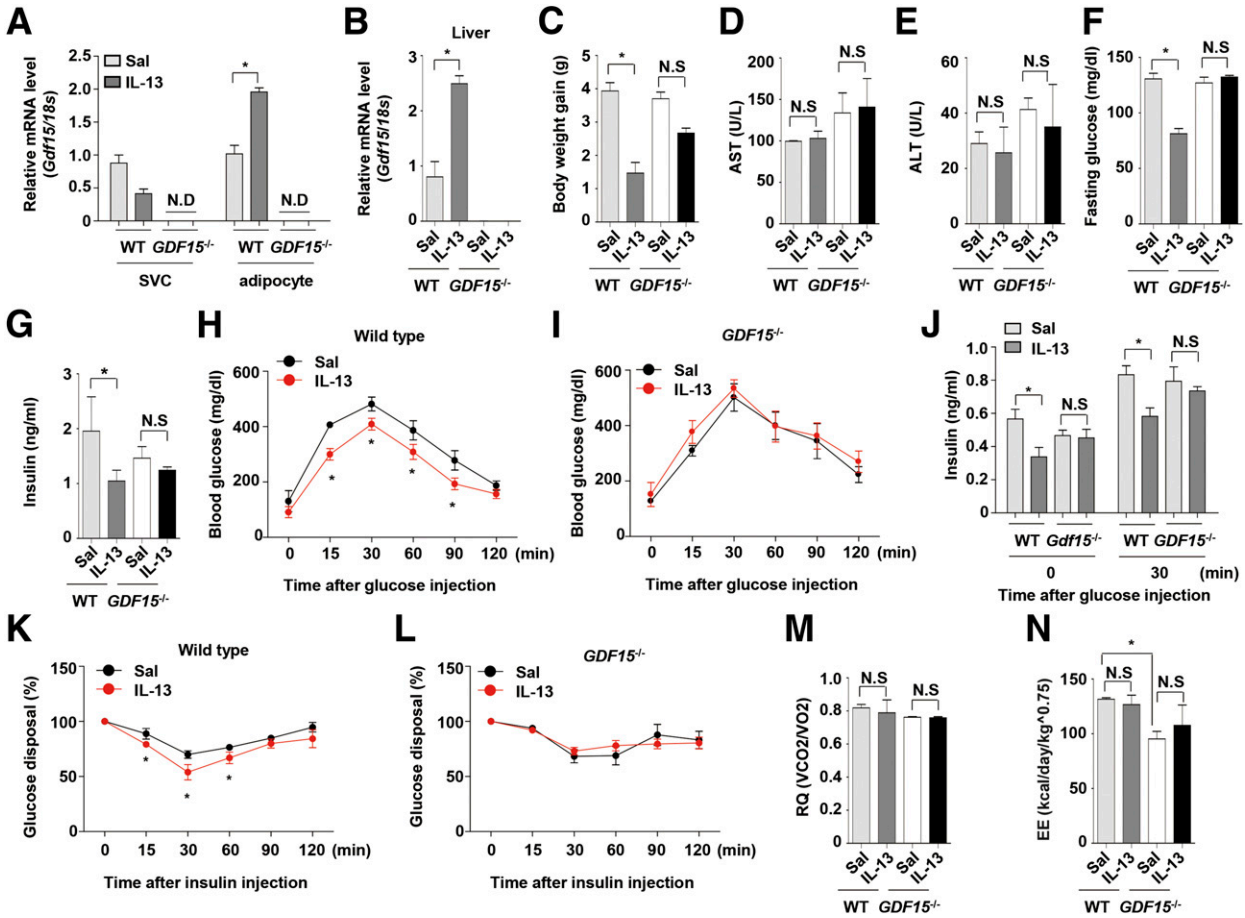

Figure 7—GDF15 is essential for IL-13–mediated amelioration of insulin resistance in HFD-fed mice. *A*: Expression of *Gdf15* mRNA expression by SVCs and adipocytes from WT and GDF15 KO mice fed an HFD and treated with recombinant IL-13 (0.5 μg; $n = 5$ per group). *B*: Hepatic *Gdf15* expression in WT and GDF15 KO mice fed an HFD and treated with recombinant IL-13. *C*: Effect of IL-13 on body weight gain by WT and GDF15 KO mice fed an HFD. *D* and *E*: Aspartate transaminase (AST) and alanine transaminase (ALT) levels in the serum of WT and GDF15 KO mice fed an HFD and treated with saline or recombinant IL-13. *F* and *G*: Effect of recombinant IL-13 on fasting blood glucose and serum insulin levels in WT and GDF15 KO mice fed an HFD. *H* and *I*: Glucose tolerance test results for WT and GDF15 KO mice fed an HFD and treated with recombinant IL-13. *J*: Plasma levels of insulin during the glucose tolerance test in WT and GDF15 KO mice treated with vehicle or recombinant IL-13. *K* and *L*: Insulin tolerance test using WT and GDF15 KO mice fed an HFD and treated with recombinant IL-13. *M* and *N*: Respiratory quotient (RQ; VCO_2/VO_2) and energy expenditure (EE) by WT and GDF15 KO mice fed an HFD and treated with saline or recombinant IL-13. All data are representative of three independent experiments and are expressed as the mean ± SEM. *$P < 0.05$ compared with the corresponding controls. N.D., not detectable; Sal, saline.

Recombinant IL-13 significantly reduced weight gain in WT mice fed the HFD but had no effect in GDF15 KO mice fed the HFD (Fig. 7*C*). In the presence of the HFD, recombinant IL-13 increased *Il13ra1* and *Il4ra1* expression in adipose tissue relative to that in saline-treated controls; however, IL-13–mediated transcription of *Il13ra1* transcription was lower in adipose tissues from GDF15 KO mice than in those from WT mice (Supplementary Fig. 8*A* and *B*). Recombinant IL-13 had no effect on aspartate transaminase and alanine transaminase levels in either group (Fig. 7*D* and *E*). Fasting glucose and insulin levels fell in WT mice treated with recombinant IL-13, but there was no significant change in GDF15 KO mice with or without recombinant IL-13 treatment (Fig. 7*F* and *G*). Recombinant IL-13 also increased glucose R_d (Fig. 7*H* and *I*) and reduced plasma insulin levels (Fig. 7*J*) in WT mice but not in GDF15 KO mice. However, glucose-induced increases in plasma insulin levels within 30 min after intraperitoneal glucose injection were similar in WT and GDF15 KO mice (Fig. 7*J*). Moreover, recombinant IL-13 did not change glucose-stimulated insulin secretion from islets (Supplementary Fig. 9). This means that IL-13 and GDF15 may not be required for glucose-induced insulin secretion by β-cells. Next, to determine the role of Th2 cytokine–induced GDF15 on insulin sensitivity, we performed an insulin tolerance test using WT and GDF15 KO mice fed the HFD. Treatment with recombinant IL-13 led to a significant improvement in insulin resistance in WT mice but not GDF15 KO mice fed the HFD (Fig. 7*K* and *L*). There were no differences in the respiratory exchange ratio and energy expenditure between the groups of mice treated with or without recombinant IL-13 (Fig. 7*M* and *N*). These data suggest that IL-13 protects effect against HFD-induced

glucose intolerance by inducing expression of GDF15 in metabolic organs.

GDF15 Is Critical for IL-13–Induced M2 Polarization of Adipose Macrophages

Previous studies show that IL-13 prevents HFD-induced weight gain and improves glucose intolerance and insulin resistance by activating M2 macrophages in murine adipose tissue (36). We therefore examined the immune cell population, including macrophages, in adipose tissue from mice treated with vehicle or recombinant IL-13. Although the difference in the T- and B-cell populations was not significant, recombinant IL-13 increased the percentage of eosinophils in adipose tissues from both groups of mice (Fig. 8*A* and *B*). To examine M1/M2 polarization of adipose macrophages in response to recombinant IL-13, we performed FACS analysis using the gating strategy described in Supplementary Fig. 10. Recombinant IL-13 reduced the number of M1 macrophages and increased that of M2 macrophages in adipose tissue from WT but not GDF15 KO mice (Fig. 8*C* and *D*). Expression of *Arg1*, *Fizz1*, and *Ym1* increased in the adipose tissue and SVC fractions from WT mice treated with recombinant IL-13 but not in those from GDF15 KO mice (Fig. 8*E–G* and Supplementary Fig. 11*A–C*). IL-13 reduced expression of *Tnfα* and *Il1β* by SVCs from WT but not GDF15 KO mice (Fig. 8*H* and *I*) and reduced expression of inducible nitric oxide synthase by adipocytes from WT mice but not by those from GDF15 KO mice

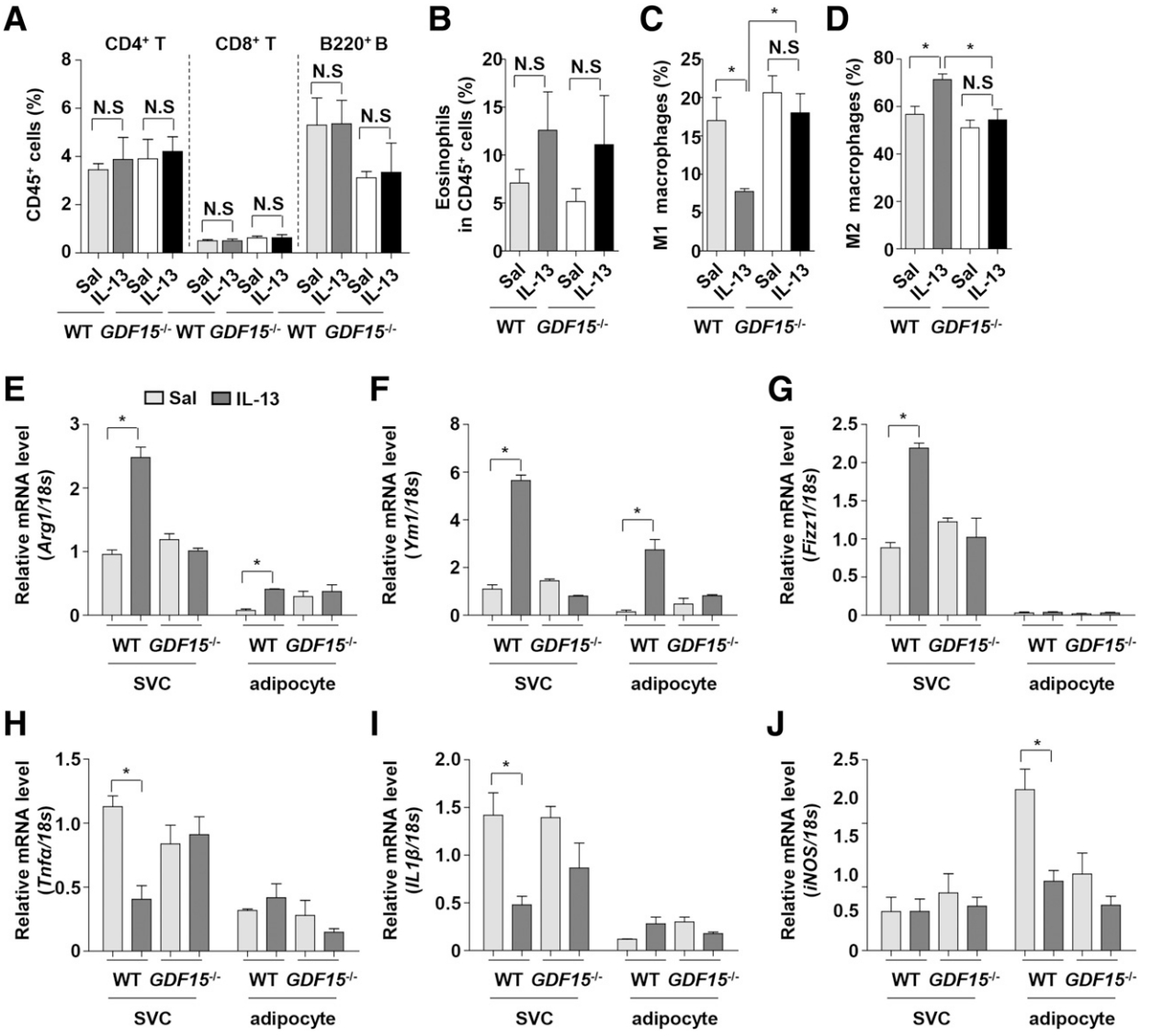

Figure 8—GDF15 is required for IL-13–induced M2 polarization of adipose macrophages. *A–D*: FACS analysis of CD4 T cell, CD8 T cell, B cell, eosinophil, M1 macrophage, and M2 macrophage populations in the eWAT of WT and GDF15 KO mice fed an HFD and treated with saline (Sal) or recombinant IL-13 (0.5 μg; $n = 5$ per group). *E–J*: Real-time PCR analysis of M1 or M2 marker gene expression by adipocytes and SVCs from WT and GDF15 KO mice treated with saline or recombinant IL-13. All results are representative of more than three independent experiments and are expressed as the mean ± SEM. *$P < 0.05$ compared with the corresponding controls.

(Fig. 8*J*). Finally, recombinant IL-13 reduced expression of *G6pase* in WT mice but not in GDF15 KO mice (Supplementary Fig. 11*D*). Collectively, these data suggest that GDF15 is essential for IL-13–mediated M2 polarization of adipose macrophages, which ultimately results in amelioration of glucose intolerance and obesity.

DISCUSSION

Recent reports show that adipose tissue functions both as an endocrine organ and as an immunological organ. Immune cells resident in adipose tissue comprise the full spectrum of innate and adaptive immune cell types, all of which play essential roles in regulating local and systemic inflammation, removing apoptotic cells and debris, and regulating tissue homeostasis (37). Obesity induced by an HFD or overnutrition results in an inflammatory microenvironment in adipose tissue, leading to deterioration of tissue-protective mechanisms that reduce the negative outcomes of immunopathology. Although the populations of immune cells, such as macrophages, mast cells, neutrophils, T cells, and B cells, increase during the development of obesity, those of eosinophils and type 2 immune cells are reduced (37,38). The regulatory function of Th2 cytokines is an important mechanism underlying systemic glucose homeostasis. IL-4 and IL-13, both induced by type 2 immune responses, reduce inflammation in adipose tissue and improve systemic glucose intolerance by inducing polarization of M2 macrophages (1,11,12). However, we lack complete understanding of how Th2 cytokines regulate expression of adipokines, which in turn regulate systemic glucose homeostasis. Here, we found that GDF15 plays a key role in Th2 cytokine–mediated immunoregulatory responses, thereby preventing metabolic deterioration caused by obesity.

In this study, we used RNA sequencing technology to identify adipokines expressed by adipocytes in the presence of IL-13. We found that IL-13 increased expression of GDF15 in cultured 3T3-L1 adipocytes and differentiated ADSCs and that GDF15 regulates systemic glucose homeostasis (Figs. 2, 7, and 8). Recombinant IL-13 improved glucose intolerance in WT mice fed the HFD but not in GDF15 KO mice fed the HFD. These data suggest that GDF15 is essential for IL-13–induced amelioration of glucose intolerance during the development of obesity caused by an HFD.

GDF15, also known as macrophage-inhibiting cytokine 1, belongs to the transforming growth factor-β superfamily and is highly expressed in the heart, liver, kidneys, and colon (39). Recent studies show that GDF15 is a stress-responsive cytokine and that its expression is elevated in obese patients and in those with prediabetes and type 2 diabetes (13,40). GDF15 is also a mitochondrial unfolded protein response–associated critical cell nonautonomous myomitokine that regulates systemic energy homeostasis by promoting oxidation and lipolysis in the liver and adipose tissues (41). Although Th2 cytokines reduce inflammation in adipose tissue and improve systemic insulin resistance, their role in GDF15 expression in adipose tissue is unclear. We found that Th2 cytokines induced GDF15 production by WT ADSCs but not by STAT6 KO ADSCs. These data suggest that STAT6 signaling is necessary for Th2 cytokine–mediated production of GDF15 by adipocytes.

STAT6 affects cellular and systemic energy metabolism (11). The STAT6 pathway is important for maintaining cellular metabolism, particularly oxidative mitochondrial metabolism. However, GDF15 increases transcriptional regulation in response to various cellular stress and metabolic changes associated with mitochondrial dysfunction (41–44). Based on these findings, we speculate that metabolic changes caused by STAT6 KO are associated with increased blood levels of GDF15. Indeed, STAT6 localizes to the mitochondria (45), possibly leading to mitochondrial dysfunction in tissues from STAT6 KO mice. This may be also associated with increased basal levels of GDF15 expression in STAT6 KO mice, although further studies are needed to confirm this. Furthermore, to exclude concerns that loss of STAT6 may induce expression of GDF15 by activating the alternative STAT pathway, we also showed that overexpression of STAT1 or STAT3 did not induce GDF15 production by adipocytes (Supplementary Fig. 4*C*). This means that activating the alternative STAT pathway may not contribute to increased basal concentrations of GDF15 in mice.

Here, we showed that Th2 cytokine–mediated production of GDF15 prevents metabolic deterioration caused by obesity. However, a recent study argues that adipose macrophages do not produce catecholamine and are therefore not implicated in adipocyte metabolism and adaptive thermogenesis (46). That study did not support the notion that macrophage production of catecholamine mediated by sIL-4–STAT6 is required for the thermogenesis or browning of WAT but did not discount the role of adipose tissue macrophages in glucose homeostasis. Here, we examined the effects of Th2 cytokine–mediated production of GDF15 and its effect on systemic glucose metabolism. We did not examine browning of WAT in mice treated with Th2 cytokines because it was beyond the scope of the study. Apart from thermogenesis or browning of adipose tissue, alternatively activated macrophages are implicated in regulation of adipose inflammation and systemic glucose homeostasis (1). We showed that STAT6-mediated GDF15 production by adipocytes plays a role in M2-like polarization of adipose tissue macrophages. Also, GDF15 increases insulin sensitivity and lipid catabolism directly (41). Taken together, these findings suggest that Th2 cytokine–mediated STAT6 activation and GDF15 release by adipocytes are important for controlling macrophage polarization and systemic glucose homeostasis.

We used two experimental murine models to examine induction of Th2 cytokines: intraperitoneal injection of αGC or recombinant IL-33. αGC-induced activation of adipose-resident iNKT cells is associated with improved systemic glucose homeostasis in obese individuals. Moreover, an abundance of adipose iNKT cells negatively correlates with BMI, insulin resistance, and fasting plasma glucose levels in humans (33). However, IL-33–mediated activation of ILC2 activates signaling pathways via eosinophil-derived

Th2 cytokines, leading to a physiological increase in beige fat biogenesis (20). Data from the two mouse models used in this study suggest that increased levels of Th2 cytokines induce GDF15 expression in adipose tissue in a STAT6-dependent manner, leading to higher levels of serum GDF15. Moreover, αGC- or IL-33–mediated reductions in fasting serum glucose levels were abolished in HFD-fed GDF15 KO mice. Therefore, the effect of Th2 cytokines on metabolic phenotype is mediated by GDF15.

We showed that short-term administration of recombinant IL-13 reduced the rate of weight gain and improved glucose tolerance during the IL-13 administration period in WT mice without altering energy expenditure and food intake; this was not the case for GDF15 KO mice (Figs. 6 and 7). However, explaining how the beneficial metabolic effects occurred in the absence of changes in energy expenditure and food consumption is difficult. We think that these metabolic benefits are produced by the direct effects of GDF15 rather than by changes in energy expenditure or feeding behavior. In addition, reduced weight gain in the absence of changes in energy expenditure and food consumption may be dependent on both the dose or treatment duration of recombinant IL-13. Several groups are currently investigating the metabolic effects of GDF15 (31,32,35,41); however, there is scant information about the signaling pathways related to the metabolic activity of GDF15. Further experiments are needed to identify the long-term benefits of IL-13 treatment.

IL-33–induced Th2 cytokines play an essential role in the proliferation of adipose tissue by controlling expansion of PDGFR-α^+ adipocyte precursors (20). Moreover, activation of Th2 cytokine signaling in adipocyte precursors regulates beige fat expansion in mice (20). Energy expenditure is also significantly decreased in PDGFR-α^+ specific IL-4Rα KO mice. However, IL-4Rα signaling in mature adipocytes does not affect the development of beige fat. Although several studies show that Th2 cytokines improve systemic glucose intolerance by regulating macrophage polarization (1,11,12), the effect of Th2 cytokines on adipokine secretion by adipocytes was not established. Here, we examined Th2 cytokines–mediated release of adipokines rather than biogenesis of beige fat or macrophage polarization. Loss-of-function studies indicated that GDF15 plays a critical role in Th2 cytokine–mediated amelioration of glucose intolerance via its effects on endocrine/systemic metabolism. Therefore, GDF15 is a novel Th2 cytokine–induced adipokine that may be a new therapeutic option for obesity and insulin resistance.

Funding. This work was supported by the Basic Science Research Program, through the National Research Foundation of Korea (NRF), funded by the Ministry of Science, ICT, and Future Planning, Korea, by NRF-2015R1A2A1A13000951, NRF-2016R1C1B1016547 (to S.-B.J.), NRF-2014R1A1A1006176 (to J.H.L.), and NRF-2015R1C1A1A01052432 (to H.-S.Y.). K.S.K. was supported by the Basic Science Research Program through NRF, funded by the Ministry of Education (NRF-2014R1A6A1029617), and the Korean Healthcare Technology R&D project, 2016 (HI16C0312).

Duality of Interest. No potential conflicts of interest relevant to this article were reported.

Author Contributions. S.E.L., S.G.K., M.J.C., S.-B.J., and M.J.R. performed the experiments and analyzed the data. S.E.L., H.-S.Y., and M.S. wrote the manuscript. H.K.C., J.Y.C., Y.K.K., J.H.L., K.S.K., H.J.K., and H.K.L. analyzed the data. H.-S.Y. and M.S. designed and supervised the research. M.S. is the guarantor of this work and, as such, had full access to all the data in the study and takes responsibility for the integrity of the data and the accuracy of the data analysis.

References

1. Wu D, Molofsky AB, Liang HE, et al. Eosinophils sustain adipose alternatively activated macrophages associated with glucose homeostasis. Science 2011;332:243–247

2. Berg AH, Scherer PE. Adipose tissue, inflammation, and cardiovascular disease. Circ Res 2005;96:939–949

3. Nishimura S, Manabe I, Nagasaki M, et al. CD8+ effector T cells contribute to macrophage recruitment and adipose tissue inflammation in obesity. Nat Med 2009;15:914–920

4. Tilg H, Moschen AR. Inflammatory mechanisms in the regulation of insulin resistance. Mol Med 2008;14:222–231

5. Fain JN, Madan AK, Hiler ML, Cheema P, Bahouth SW. Comparison of the release of adipokines by adipose tissue, adipose tissue matrix, and adipocytes from visceral and subcutaneous abdominal adipose tissues of obese humans. Endocrinology 2004;145:2273–2282

6. Kern PA, Ranganathan S, Li C, Wood L, Ranganathan G. Adipose tissue tumor necrosis factor and interleukin-6 expression in human obesity and insulin resistance. Am J Physiol Endocrinol Metab 2001;280:E745–E751

7. Feuerer M, Herrero L, Cipolletta D, et al. Lean, but not obese, fat is enriched for a unique population of regulatory T cells that affect metabolic parameters. Nat Med 2009;15:930–939

8. Winer S, Chan Y, Paltser G, et al. Normalization of obesity-associated insulin resistance through immunotherapy. Nat Med 2009;15:921–929

9. Brestoff JR, Kim BS, Saenz SA, et al. Group 2 innate lymphoid cells promote beiging of white adipose tissue and limit obesity. Nature 2015;519:242–246

10. Miller AM, Asquith DL, Hueber AJ, et al. Interleukin-33 induces protective effects in adipose tissue inflammation during obesity in mice. Circ Res 2010;107:650–658

11. Ricardo-Gonzalez RR, Red Eagle A, Odegaard JI, et al. IL-4/STAT6 immune axis regulates peripheral nutrient metabolism and insulin sensitivity. Proc Natl Acad Sci U S A 2010;107:22617–22622

12. Stanya KJ, Jacobi D, Liu S, et al. Direct control of hepatic glucose production by interleukin-13 in mice. J Clin Invest 2013;123:261–271

13. Ding Q, Mracek T, Gonzalez-Muniesa P, et al. Identification of macrophage inhibitory cytokine-1 in adipose tissue and its secretion as an adipokine by human adipocytes. Endocrinology 2009;150:1688–1696

14. Cai Y, Zhou J, Webb DC. Estrogen stimulates Th2 cytokine production and regulates the compartmentalisation of eosinophils during allergen challenge in a mouse model of asthma. Int Arch Allergy Immunol 2012;158:252–260

15. Riffo-Vasquez Y, Ligeiro de Oliveira AP, Page CP, Spina D, Tavares-de-Lima W. Role of sex hormones in allergic inflammation in mice. Clin Exp Allergy 2007;37:459–470

16. Estes BT, Diekman BO, Gimble JM, Guilak F. Isolation of adipose-derived stem cells and their induction to a chondrogenic phenotype. Nat Protoc 2010;5:1294–1311

17. Trapnell C, Pachter L, Salzberg SL. TopHat: discovering splice junctions with RNA-Seq. Bioinformatics 2009;25:1105–1111

18. Trapnell C, Williams BA, Pertea G, et al. Transcript assembly and quantification by RNA-Seq reveals unannotated transcripts and isoform switching during cell differentiation. Nat Biotechnol 2010;28:511–515

19. Lynch L, Michelet X, Zhang S, et al. Regulatory iNKT cells lack expression of the transcription factor PLZF and control the homeostasis of T(reg) cells and macrophages in adipose tissue. Nat Immunol 2015;16:85–95

20. Lee MW, Odegaard JI, Mukundan L, et al. Activated type 2 innate lymphoid cells regulate beige fat biogenesis. Cell 2015;160:74–87
21. Aman MJ, Tayebi N, Obiri NI, Puri RK, Modi WS, Leonard WJ. cDNA cloning and characterization of the human interleukin 13 receptor alpha chain. J Biol Chem 1996; 271:29265–29270
22. Idzerda RL, March CJ, Mosley B, et al. Human interleukin 4 receptor confers biological responsiveness and defines a novel receptor superfamily. J Exp Med 1990; 171:861–873
23. David M, Ford D, Bertoglio J, Maizel AL, Pierre J. Induction of the IL-13 receptor alpha2-chain by IL-4 and IL-13 in human keratinocytes: involvement of STAT6, ERK and p38 MAPK pathways. Oncogene 2001;20:6660–6668
24. Renz H, Domenico J, Gelfand EW. IL-4-dependent up-regulation of IL-4 receptor expression in murine T and B cells. J Immunol 1991;146:3049–3055
25. Yanagihara Y, Ikizawa K, Kajiwara K, Koshio T, Basaki Y, Akiyama K. Functional significance of IL-4 receptor on B cells in IL-4-induced human IgE production. J Allergy Clin Immunol 1995;96:1145–1151
26. Bhattacharjee A, Shukla M, Yakubenko VP, Mulya A, Kundu S, Cathcart MK. IL-4 and IL-13 employ discrete signaling pathways for target gene expression in alternatively activated monocytes/macrophages. Free Radic Biol Med 2013;54:1–16
27. Wery-Zennaro S, Letourneur M, David M, Bertoglio J, Pierre J. Binding of IL-4 to the IL-13Ralpha(1)/IL-4Ralpha receptor complex leads to STAT3 phosphorylation but not to its nuclear translocation. FEBS Lett 1999;464:91–96
28. Kim HJ, Kim CH, Lee DH, et al. Expression of eotaxin in 3T3-L1 adipocytes and the effects of weight loss in high-fat diet induced obese mice. Nutr Res Pract 2011;5: 11–19
29. Sharma R, Colarusso P, Zhang H, Stevens KM, Patel KD. FRNK negatively regulates IL-4-mediated inflammation. J Cell Sci 2015;128:695–705
30. Richard AJ, Stephens JM. Emerging roles of JAK-STAT signaling pathways in adipocytes. Trends Endocrinol Metab 2011;22:325–332
31. Chrysovergis K, Wang X, Kosak J, et al. NAG-1/GDF-15 prevents obesity by increasing thermogenesis, lipolysis and oxidative metabolism. Int J Obes 2014;38: 1555–1564
32. Macia L, Tsai VW, Nguyen AD, et al. Macrophage inhibitory cytokine 1 (MIC-1/GDF15) decreases food intake, body weight and improves glucose tolerance in mice on normal & obesogenic diets. PLoS One 2012;7:e34868
33. Ji Y, Sun S, Xu A, et al. Activation of natural killer T cells promotes M2 Macrophage polarization in adipose tissue and improves systemic glucose tolerance via interleukin-4 (IL-4)/STAT6 protein signaling axis in obesity. J Biol Chem 2012; 287:13561–13571
34. Kurowska-Stolarska M, Kewin P, Murphy G, et al. IL-33 induces antigen-specific IL-5+ T cells and promotes allergic-induced airway inflammation independent of IL-4. J Immunol 2008;181:4780–4790
35. Wang X, Chrysovergis K, Kosak J, et al. hNAG-1 increases lifespan by regulating energy metabolism and insulin/IGF-1/mTOR signaling. Aging (Albany NY) 2014; 6:690–704
36. Molofsky AB, Nussbaum JC, Liang HE, et al. Innate lymphoid type 2 cells sustain visceral adipose tissue eosinophils and alternatively activated macrophages. J Exp Med 2013;210:535–549
37. Mraz M, Haluzik M. The role of adipose tissue immune cells in obesity and low-grade inflammation. J Endocrinol 2014;222:R113–R127
38. Cildir G, Akıncılar SC, Tergaonkar V. Chronic adipose tissue inflammation: all immune cells on the stage. Trends Mol Med 2013;19:487–500
39. Bootcov MR, Bauskin AR, Valenzuela SM, et al. MIC-1, a novel macrophage inhibitory cytokine, is a divergent member of the TGF-beta superfamily. Proc Natl Acad Sci USA 1997;94:11514–11519
40. Kempf T, Guba-Quint A, Torgerson J, et al. Growth differentiation factor 15 predicts future insulin resistance and impaired glucose control in obese nondiabetic individuals: results from the XENDOS trial. Eur J Endocrinol 2012;167: 671–678
41. Chung HK, Ryu D, Kim KS, et al. Growth differentiation factor 15 is a myomitokine governing systemic energy homeostasis. J Cell Biol 2017;216:149–165
42. Li PX, Wong J, Ayed A, et al. Placental transforming growth factor-beta is a downstream mediator of the growth arrest and apoptotic response of tumor cells to DNA damage and p53 overexpression. J Biol Chem 2000;275:20127–20135
43. Sasahara A, Tominaga K, Nishimura T, et al. An autocrine/paracrine circuit of growth differentiation factor (GDF) 15 has a role for maintenance of breast cancer stem-like cells. Oncotarget 2017;8:24869–24881
44. Varadarajan S, Breda C, Smalley JL, et al. The transrepression arm of glucocorticoid receptor signaling is protective in mutant Huntington-mediated neurodegeneration. Cell Death Differ 2015;22:1388–1396
45. Khan R, Lee JE, Yang YM, Liang FX, Sehgal PB. Live-cell imaging of the association of STAT6-GFP with mitochondria. PLoS One 2013;8:e55426
46. Fischer K, Ruiz HH, Jhun K, et al. Alternatively activated macrophages do not synthesize catecholamines or contribute to adipose tissue adaptive thermogenesis. Nat Med 2017;23:623–630